FEBS Letters

FEBS PRESS science publishing by scientists

Ablation of fatty acid desaturase 2 (FADS2) exacerbates hepatic triacylglycerol and cholesterol accumulation in polyunsaturated fatty acid-depleted mice

Yuri Hayashi[1], Hyeon-Cheol Lee-Okada[2], Eri Nakamura[3], Norihiro Tada[3], Takehiko Yokomizo[2], Yoko Fujiwara[4,5] and Ikuyo Ichi[4,5]

1 Graduate School of Humanities and Sciences, Ochanomizu University, Tokyo, Japan
2 Department of Biochemistry, Juntendo University Graduate School of Medicine, Tokyo, Japan
3 Laboratory of Genome Research, Research Institute for Diseases of Old Age, Juntendo University Graduate School of Medicine, Tokyo, Japan
4 Institute for Human Life Innovation, Ochanomizu University, Tokyo, Japan
5 Natural Science Division, Faculty of Core Research, Ochanomizu University, Tokyo, Japan

Correspondence
I. Ichi, Natural Science Division, Faculty of Core Research, Ochanomizu University, Otsuka 2-1-1, Bunkyo-ku, Tokyo 112-8610, Japan
Tel: +81 3 5978 5750
E-mail: ichi.ikuyo@ocha.ac.jp

Requests for the FADS2 knockout mice should be addressed to HCLO (h-lee@juntendo.ac.jp) or TY (yokomizo-tky@umin.ac.jp)

(Received 6 February 2021, revised 22 April 2021, accepted 10 May 2021, available online 1 June 2021)

doi:10.1002/1873-3468.14134

Edited by László Nagy

Deficiency of polyunsaturated fatty acids (PUFAs) is known to induce hepatic steatosis. However, it is not clearly understood which type of PUFA is responsible for the worsening of steatosis. This study observed a marked accumulation of hepatic triacylglycerol and cholesterol in fatty acid desaturase 2 knockout (FADS2$^{-/-}$) mice lacking both C18 and ≥ C20 PUFAs that were fed a PUFA-depleted diet. Hepatic triacylglycerol accumulation was associated with enhanced sterol regulatory element-binding protein (SREBP)-1-dependent lipogenesis and decreased triacylglycerol secretion into the plasma via very-low-density lipoprotein (VLDL). Furthermore, upregulation of cholesterol synthesis contributed to increased hepatic cholesterol content in FADS2$^{-/-}$ mice. These results suggest that ≥ C20 PUFAs synthesized by FADS2 are important in regulating hepatic triacylglycerol and cholesterol accumulation during PUFA deficiency.

Keywords: cholesterol; fatty acid desaturase; hepatic steatosis; highly unsaturated fatty acids; lipogenesis; polyunsaturated fatty acid

Polyunsaturated fatty acids (PUFAs) play an important role in determining the structure and integrity of biological membranes and generate bioactive lipids that mediate numerous physiological functions. Mammals are unable to synthesize n-6 and n-3 PUFAs de novo and must obtain these PUFAs from the diet; this is why linoleic acid (18:2n-6) and α-linolenic acid (18:3n-3) are called essential fatty acids (EFAs). Highly unsaturated fatty acids (HUFAs; ≥ 20 carbons and ≥ 3 double bonds) such as 20:4n-6 (arachidonic acid), 20:5n-3 (eicosapentaenoic acid; EPA), and 22:6n-3 (docosahexaenoic acid; DHA) can be synthesized from EFAs (Fig. 1). In dietary n-6 and n-3 PUFA-deficient mammals, Mead acid (20:3n-9) is endogenously produced from oleic acid (18:1n-9) and used as a diagnostic indicator of EFA-deficiency [1]. We previously reported that Mead acid is produced from oleic acid via two desaturase enzymes (FADS1 and FADS2) and

Abbreviations
EFA, essential fatty acid; FADS, fatty acid desaturase; FASN, fatty acid synthase; HDL, high-density lipoprotein; HMGCR, HMG-CoA reductase; HUFA, highly unsaturated fatty acid; KO, knockout; LXR, liver X receptor; PC, phosphatidylcholine; PUFA, polyunsaturated fatty acid; SCD, stearoyl-CoA desaturase; SREBP, sterol regulatory element-binding protein; TAG, triacylglycerol; VLDL, very low-density lipoprotein; WT, wild type.

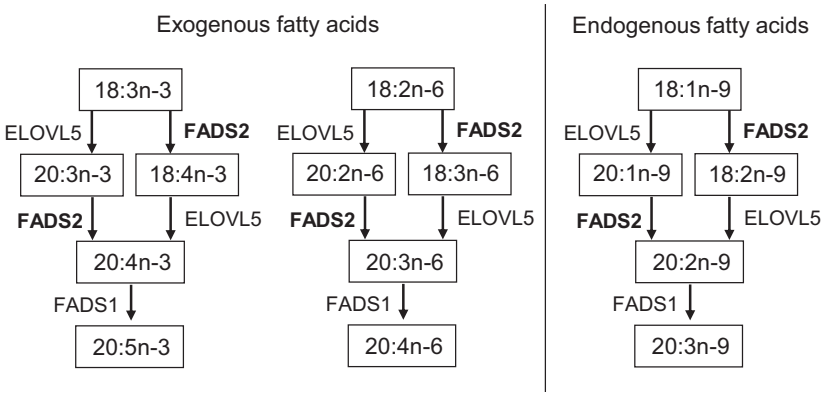

Fig. 1. The mammalian synthetic pathway of exogenous and endogenous PUFAs.

one elongase enzyme (ELOVL5), indicating that the same enzymes are involved in the synthesis of n-3, n-6, and n-9 HUFAs (Fig. 1) [2]. Arachidonic acid (20:4n-6), an exogenous n-6 HUFA in membrane phospholipids, is required to transport lipids from the liver to the plasma [3,4]. Our previous study indicated that Mead acid in phospholipids might similarly rescue the impaired hepatic lipid transport during EFA-deficiency [5], further suggesting that Mead acid could be used as a substitute for exogenous HUFAs in biological membranes. In addition, the oxidative metabolites of Mead acid are reported to participate in both proinflammatory [6] and anti-inflammatory signaling pathways [7].

Dietary PUFA deprivation is found in patients with intestinal malabsorption of lipids [8] and patients receiving no fat during total parenteral nutrition [9]. The symptoms of PUFA deficiency have been reported to include impaired growth, skin lesions, infertility, and hepatic steatosis [10]. Hepatic steatosis is caused by excessive accumulation of neutral lipids such as triacylglycerol (TAG) and cholesterol ester in hepatocytes. PUFA-depleted diet has been reported to lead to hepatic TAG accumulation in mice via activated liver X receptor (LXR)-sterol regulatory element-binding protein (SREBP)-1c [11] and via inhibited secretion of very-low-density lipoprotein (VLDL) particles [12]. However, it is unknown which of the EFAs (C18 PUFAs) or the derivatives of EFAs (≥ C20 PUFAs) are responsible for the increase in hepatic TAG content when PUFAs are deficient. Moreover, although excessive cholesterol accumulation in the liver has been shown to aggravate the pathogenesis of steatosis [13], it is unclear whether dietary PUFA deprivation causes increased hepatic cholesterol content.

Fatty acid desaturase 2 (FADS2) is the first and rate-limiting enzyme in the biosynthesis of n-3 and n-6 HUFAs (Fig. 1). Dysfunction of FADS2 results in the lack of ≥ C20 PUFAs production from C18 PUFAs because there is no other isoform of delta 6-desaturase that can act on 18-carbon unsaturated fatty acids [14,15]. FADS2 knockout mice (FADS2$^{-/-}$) are known to exhibit pathologies such as dysfunction of spermiogenesis, ulcerative dermatitis, and ulceration in the duodenum and ileocecal junction [14,15]. Furthermore, it has been reported that hepatic steatosis is observed in FADS2$^{-/-}$ mice fed a diet including C18 PUFA but not ≥ C20 PUFAs and shown to be alleviated by the administration of arachidonic acid [16]. Our previous study showed that normal mice fed a PUFA-deficient diet had a marked decrease in C18 PUFAs in the liver, but only a slight decrease in ≥ C20 PUFAs [5]. However, the significance of the maintenance of ≥ C20 PUFAs in the mice fed a PUFA-deficient diet is unclear. Since FADS2 is also involved in the synthesis of Mead acid from oleic acid, we speculate that the levels of both exogenous ≥ C20 PUFAs and Mead acid are reduced in FADS2$^{-/-}$ mice fed a diet without PUFAs. This study investigated the effects of inhibition of the synthesis of exogenous and endogenous ≥ C20 PUFAs during EFA-deficiency on the hepatic accumulation of TAG and cholesterol using FADS2$^{-/-}$ mice. We also studied the underlying mechanisms of hepatic accumulation of these neutral lipids in FADS2-deficient mice.

Materials and methods

Generation of FADS2$^{-/-}$ mice

FADS2$^{-/-}$ mice were generated using the CRISPR/Cas9 system [17] at Juntendo University. Cas9 mRNA (100 ng·μL^{-1}) and sgRNA (40 ng·μL^{-1}) were microinjected into the cytoplasm of fertilized one-cell eggs at the pronuclei stage from C57BL/6J female mice (Charles River Laboratories Japan, Inc., Yokohama, Japan) superovulated by the intraperitoneal injection of PMSG followed by hCG at an interval of 48 h and mated overnight with C57BL/6J male mice (Charles River Laboratories Japan, Inc.).

Microinjections were performed by micromanipulators (Leica, Wetzlar, Germany) with a PMM-150 FU piezo-impact drive unit (Prime Tech Inc., Ibaragi, Japan) using a blunt-ended mercury-containing injection pipette with an inner diameter of approximately 6 μm [18]. After microinjection, two-cell stage embryos were cultured in modified Whitten's medium (Mitsubishi Kagaku Iatron Inc., Tokyo, Japan) for approximately 24 h. After developing from fertilized one-cell eggs, they were transferred into the oviducts of pseudopregnant ICR females (Charles River Laboratories Japan, Inc.) at 0.5 dpc. Mice were fed *ad libitum* with a standard diet and maintained in an air-conditioned and light-controlled animal room (23 °C ± 1 °C, 55% ± 5%, 12-h light/12-h dark). All animal experiments were performed following the Guidelines of Laboratory Animal Experimentation at Juntendo University and approved by the Institutional Animal Care and Use Committee at Juntendo University.

Mutations were evaluated by polymerase chain reaction (PCR) followed by a T7E1 enzyme assay. The sequence of sgRNA used for FADS2$^{-/-}$ mouse generation is 5′-CTCCGATGCCCACCTTCCGTTGG-3′. Genomic DNA was extracted from the tail chips of FADS2$^{-/-}$ with DNeasy Blood & Tissue Kit (Qiagen, Hilden, Germany), following the manufacturer's instructions. PCR conditions were 98 °C for 10 s, 60 °C for 30 s, and 72 °C for 1 min for 30 cycles (1st PCR) and 35 cycles (2nd PCR). Primer sequences used in the genotyping of FADS2$^{-/-}$ mice are indicated below. Fads2 F_1st: 5′-CCAGCAGGGCTTAA CTCCA-3′; Fads2 R_1st: 5′-CTCCCGAATAGTGTC CGATG-3′; Fads2 F_2nd: 5′-GCTCTGCTGATCAC TGTGGAA-3′; Fads2 R_2nd: 5′-TGTAGACCTT GCGGTCGATG-3′. Annealed PCR products were treated with T7 endonuclease to evaluate mismatches at the target site. The PCR products were column-purified using NucleoSpin Gel and PCR Clean-up (MACHEREY-NAGEL, Düren, Germany). TA was cloned using pGEM®T-Easy Vector System I (Promega, Madison, WI, USA) and sequenced to determine the mutations. Consequently, two strains of FADS2$^{-/-}$ mice were established. The first strain possessed a 65 bp deletion downstream of the start codon (frameshift mutation), and the second strain possessed an 81 bp deletion that includes the start codon (Fig. S1). These mice were backcrossed onto the C57BL/6J background for at least two generations prior to biochemical and lipidomic analyses. Neither strain expresses functional FADS2 protein, and they show almost the same lipidomic changes and phenotypes (data not shown). In the present study, the second strain was used for further analyses.

Animal experiments

FADS2$^{-/-}$ mice were obtained by heterozygous mating. After mating, these mice were distinguished from FADS2$^{+/-}$ and FADS2$^{+/+}$ mice by PCR using forward (F-5'-GCTAGCTAGTGAAGGCGAGG-3') and reverse (5'-TGTAGACCTTGCGGTCGATG-3') primers (Fig. S1C). Male FADS2$^{-/-}$ mice and littermate wild type (WT) mice were housed under controlled temperature and humidity and under a 12:12-h dark-light cycle. The FADS2$^{-/-}$ mice (10 weeks old) were fed a PUFA-deficient diet for 4 weeks and designated as KO-DEF mice. In addition, 10-week-old WT mice were fed a control diet (WT-CONT) or PUFA-deficient diet (WT-DEF) for 4 weeks. The control diet was AIN-93G containing 7% soybean oil as the lipid source, and the PUFA-deficient diet was AIN-93G with 7% tripalmitate (Tokyo Chemical Industry, Japan) substituted for soybean oil. Mice were anesthetized and sacrificed by collecting blood from the heart. After perfusion with physiological saline through the heart, the liver was removed. Blood was centrifuged at 3 000 ***g*** for 10 min at 4 °C to separate the plasma. The liver and plasma were stored at −80 °C until further analysis. This study was carried out in accordance with the recommendations in the Guide for the Care and Use of Laboratory Animals of the National Institutes of Health. The protocol was approved by the Committee on the Ethics of Animal Experiments of Ochanomizu University.

Lipid analysis

Lipids were extracted from plasma and liver using the method described by Bligh and Dyer [19]. The TAG concentrations in the plasma and liver were quantified using the Triglyceride E-Test Wako Kit (Wako Pure Chemicals, Osaka, Japan). The cholesterol concentration in plasma and bile was quantified using LabAssay™ Cholesterol (Wako Pure Chemicals). For fatty acid analysis, extracted lipids were methylated with 2.5% H_2SO_4 in methanol. The fatty acid methyl esters were then extracted with *n*-hexane and quantified by gas chromatography-mass spectrometry (GC/MS) using a GC/MS QP2010 (Shimadzu, Kyoto, Japan), as described previously [20]. The phospholipids were separated by thin-layer chromatography (Merck Millipore, Darmstadt, Germany), and then fatty acids in phosphatidylcholine (PC) were methylated and measured by GC/MS. For cholesterol analysis, hepatic lipids were allowed to saponify at 70 °C for 1 h and were extracted with *n*-hexane three times. Oxysterols were measured as previously described [21]. Lipids were extracted from the liver, and the lipids were saponified at room temperature overnight in the dark. Unsaponified lipids were applied to a Sep-Pak Vac silica cartridge (Waters) to separate oxysterols and sterols [22]. Cholesterol or separated oxysterols were converted into trimethylsilyl ethers in a mixture of trimethylchlorosilane, 1,1,1,3,3,3-hexamethyldisilazane, and dried pyridine (1 : 3 : 9, v : v : v) for 30 min at room temperature. Sterols were quantified by GC/MS equipped with an SPB-1 fused silica capillary column of 60 m × 0.25 mm and 0.25 μm phase thickness (Supelco Inc., Bellefonte, PA,

USA). The total bile acid (TBA) content in the plasma was analyzed by Oriental Kobo Co. (Tokyo, Japan).

Lipoprotein analysis

Plasma lipoproteins were analyzed using an on-line dual enzymatic method for the simultaneous quantification of cholesterol and TAG in lipoproteins by high-performance liquid chromatography (HPLC) at Skylight Biotech (Akita, Japan), following a previously described procedure [23].

H&E staining of liver sections

Formalin-fixed liver tissue was embedded in paraffin, sliced, and stained with H&E using a standard protocol.

Total RNA isolation and quantitative real-time PCR

Total RNA was extracted from tissues using TRIzol™ Reagent (Invitrogen, Carlsbad, CA, USA) and reverse-transcribed using a High Capacity cDNA Reverse Transcription kit (Applied Biosystems, Foster City, CA, USA). Quantitative real-time PCR was performed using SYBR™ Green PCR Master Mix and 7300 Real-Time PCR System (Applied Biosystems). The relative target gene expression was normalized to that of β-actin in the liver or Gapdh in the intestine. The DNA oligo primers used are shown in Table 1.

Western blot analysis

Equal amounts of protein were separated by sodium dodecyl sulfate-polyacrylamide gel electrophoresis (SDS/PAGE), transferred to Immobilon PVDF membranes, and probed with anti-SREBP-1 (2A4) (Santa Cruz Biotechnology, Santa Cruz, CA, USA), apolipoprotein B (Abcam, Cambridge, UK), and SREBP-2 (1C6) (Santa Cruz Biotechnology) antibodies. The secondary antibodies used were anti-mIgGκ BP antibody (Santa Cruz Biotechnology) and goat anti-rabbit antibody (Jackson ImmunoResearch, West Grove, PA, USA) conjugated to horseradish peroxidase. Immunoreactive bands were visualized by enhanced chemiluminescence (GE Healthcare, Waukesha, WI, USA).

Table 1. Primer sequences used in the qRT-PCR assays.

Target	Forward primer sequence	Reverse primer sequence
Beta-actin	GCCAACCGTGAAAAGATGAC	CCAGAGGCATACAGGGACAG
Gapdh	GCCAAGGTCATCCATGACAACT	GAGGGGCCATCCACAGTCTT
Acc	GAAAATCCACAATGCCAACC	TTGCTTCTCCAGCCACTCC
Scd1	TACACCTGCCTCTTCGGGATT	GCCGTGCCTTGTAAGTTCTGT
Mcad	GCAGAGAAGAAGGGTGACGAG	CGTGCCAACAAGAAATACCAG
Insig-1	GTCCTGGGTGTGATGAAGATG	GTGGGGGAGCAAGGTAAGAC
Insig-2a	CCCTCAATGAATGTACTGAAGGATT	TGTGAAGTGAAGCAGACCAATGT
Srebf-1c	AAGCTGTCGGGGTAGCGTCT	CTTGGTTGTTGATGAGCTGGAG
Fasn	TTGCCCGAGTCAGAGAACC	ATAGAGCCCAGCCTTCCATC
Cpt1a	CAACAACGGCAGAGCAGAG	GGACACCACATAGAGGCAGAAG
Mcad	GCAGAGAAGAAGGGTGACGAG	CGTGCCAACAAGAAATACCAG
Mttp	AAATCGGGTGGCTGTGG	TCTGTCTCCGCTCTGCTTTC
Cd36	AGAACAGCAGCAAAATCAAGGT	GACAGTGAAGGCTCAAAGATGG
Fatp2	TGAATGTGTATGGCGTGCCT	AGGTACTCCGCGATGTGTTG
Fatp5	TGGATCCAGACCTCCAGGAG	TCAGAAGGTGCAGCATCCAG
Srebf-2	GACCAGCACCCATACTCAGG	CACCATTTACCAGCCACAGG
Hmgcr	CCAGGAGCGAACCAAGAGAG	CAGAAGCCCCAAGCACAAAC
Fdps	GACGGCTTTCTACTCTTTCTACCTG	GCATTGGCGTGTTCCTTC
Sqls	GCAAAACCAAGCAGGTCATC	GACAGGTAAATGGGGGAGTAGTG
Lss	GATTTTCCCCTTCTCTCCTGAC	ACACTGAACGCCTCTCCATC
Ldlr	GACCCAGAGCCATCGTAGTG	CACCATTCAAACCCCCTTTC
Abca1	ACAGAAAACCGCAGACATCC	AAACCCGCCATACCGAAAC
Pcsk9	TGTCTATGCTTCCTGCTGCC	GTGACCTGCTCTGAAGGACC
Scarb1	TGGGGTCTTCACTGTCTTCAC	ATCTTGCTGAGTCCGTTCCA
Apo-a1	TGTATGTGGATGCGGTCAAAG	ACCCAGAGTGTCCCAGTTTTC
Cyp7a1	TGTCCACTTCATCACAAACTCC	CATCACTTGGGTCTATGCTTCTG
Cyp27a1	GCTATGGGGTTCGGTCTTG	ATGCGGGACACAGTCTTTACTTC
Abcg5	GCTGAGGCGAGTAACAAGAAAC	GCGGAGAAGGTAGAAAATGAGG
Abcg8	AGGCAAAGGAACTCAACACAAG	CAGGGTGGAAAACTGCTCTATC
Npc1l1	TCCAGAACAACCACACACTCC	GCATTGGCACAGTAGAGGAAA

Measurement of plasma PCSK9 concentration

Plasma PCSK9 concentration was measured using Mouse/Rat PCSK9 ELISA kit from CircuLex (CircuLex CycLex Co., Ltd., Nagano, Japan) according to manufacturer's protocol.

Statistical analysis

Values are presented as mean ± standard error (SE) with 5–6 mice per group. Statistical significance was determined using the Tukey–Kramer test to identify significant differences ($P < 0.05$).

Results

The hepatic PUFA composition in FADS2 knockout mice fed a PUFA-deficient diet

We generated FADS2$^{-/-}$ mice using the CRISPR/Cas9 system (Fig. S1). In FADS2$^{-/-}$ mice fed a PUFA-deficient diet (KO-DEF), the de novo synthesized fatty acids such as 16:0, 18:1n-9, and 20:1n-9 were markedly increased in the liver (Fig. 2A,B). The Mead acid level was increased in the liver of the WT mice fed a PUFA-deficient diet (WT-DEF) but was not detected in the KO-DEF group (Fig. 2B), showing that the production of Mead acid was completely suppressed in FADS2$^{-/-}$ mice. Exogenous fatty acid, 18:2n-6 in the two groups fed a PUFA-deficient diet were reduced to less than half that in the WT-CONT group, whereas no further reduction was observed in the KO-DEF group (Fig. 2C). However, ≥ C20 PUFAs such as 20:3n-6, 20:4n-6, and 22:6n-3 were significantly decreased in the KO-DEF group compared with those in the other two groups (Fig. 2C). Similarly, the total amount of C18 PUFAs (18:2n-6 and 18:3n-3) was decreased in the two groups of mice fed a PUFA-deficient diet (Fig. 2D). Furthermore, the total amount of ≥ C20 PUFAs (20:3n-6, 20:3n-9, 20:4n-6, 20:5n-3, 22:5n-3, and 22:6n-3) was dramatically diminished in the KO-DEF group (Fig. 2D). A remarkable decrease of total ≥ C20 PUFA levels was also found in the plasma of the KO-DEF group (Fig. S2). Thus, we confirmed that FADS2 knockout mice fed a PUFA-free diet exhibited a marked reduction of both C18 and ≥ C20 PUFAs.

The hepatic lipid accumulation in FADS2 knockout mice fed a PUFA-deficient diet

Although there was no difference in body weight among the three groups (data not shown), the liver weight of the KO-DEF group was significantly higher than that of the other two groups (Fig. 2E).

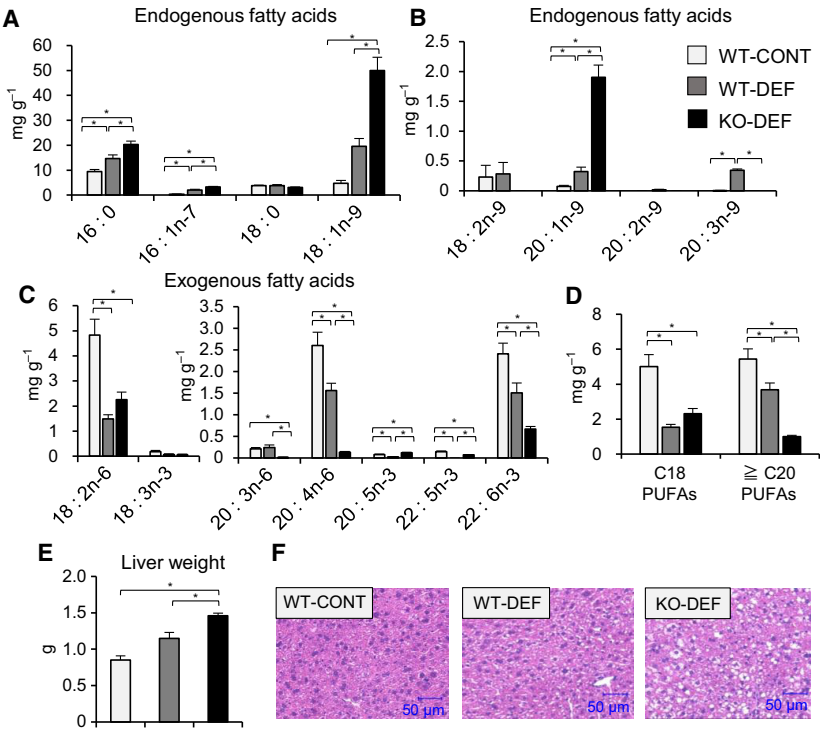

Fig. 2. PUFA-deficient FADS2$^{-/-}$ mice exhibited a reduction of ≥ C20 PUFA levels and hepatic lipid accumulation. (A–D) The fatty acid compositions in the liver of *FADS2*$^{-/-}$ mice (KO-DEF), WT mice (WT-DEF) fed a PUFA-deficient diet, and WT mice (WT-CONT) fed a control diet were determined by GC-MS. The amounts of (A, B) endogenous fatty acids, (C) exogenous fatty acids, (D) total amounts of C18 PUFA (18:2n-6 and 18:3n-3) and ≥ C20 PUFAs (20:3n-6, 20:3n-9, 20:4n-6, 20:5n-3, 22:5n-3, and 22:6n-3). (E) The liver weight was determined. (F) Liver sections of KO-DEF, WT-DEF, and WT-CONT mice stained with hematoxylin and eosin (H&E). Data are presented as mean values ± SE of 5–6 mice per group; *$P < 0.05$.

Hematoxylin and eosin staining of liver sections revealed a slight increase in hepatic lipid droplets in the WT-DEF group compared with the WT-CONT group, while the number of large droplets in the KO-DEF group was greater than those in the other two groups (Fig. 2F). Thus, the accumulation of neutral lipids was observed in the liver of FADS2$^{-/-}$ mice with the marked decrease of ≥ C20 PUFAs. To examine whether genetic FADS2 deficiency itself caused hepatic steatosis, WT or FADS2$^{-/-}$ mice were fed the high sucrose diet containing soybean oil for 4 weeks to induce fatty liver. Total ≥ C20 PUFAs content in the liver of FADS2$^{-/-}$ mice fed the soybean oil diet remained about 50% of that in WT mice (Fig. S3A). The liver weight of FADS2$^{-/-}$ mice fed the soybean oil diet was similar to that of WT mice (Fig. S3B), and hematoxylin and eosin staining showed that the liver from FADS2$^{-/-}$ mice had only a slight increase of lipid droplets compared with that from WT mice (Fig. S3C). Based on these results, we investigated the causes behind the hepatic steatosis in FADS2$^{-/-}$ mice fed the PUFA-deficient diet.

The increase of hepatic lipogenesis in FADS2 knockout mice fed a PUFA-deficient diet

KO mice fed the DEF diet showed a significant increase of hepatic TAG level compared to two groups of WT mice (Fig. 3A). To reveal the effect of deprivation of exogenous and endogenous HUFA on the synthesis of TAG in the liver, we examined the expression of genes involved in fatty acid synthesis. The hepatic expression levels of fatty acid synthase (*Fasn*), stearoyl-CoA desaturase (*Scd*), and acetyl-CoA carboxylase (*Acc*) were significantly increased in the KO-DEF group compared with those in the WT-CONT. There were no significant differences found between the WT-CONT and WT-DEF groups (Fig. 3B). In addition, sterol regulatory element-binding factor-1c (*Srebf-1c*) is the transcription factor of fatty acid synthesis genes. Insulin-induced gene-1 (*Insig-1*) is also a target gene of SREBP-1 and interacts with SREBPs in ER to retain full-length SREBPs [24]. The expression of these genes was significantly elevated in the KO-DEF group compared with that of the other two groups, whereas the expression level of *Insig-2a* was only mildly elevated (Fig. 3B) The expression of carnitine palmitoyltransferase 1A (*Cpt1a*), a gene related to fatty acid oxidation, was significantly increased in the KO-DEF group compared to the other two groups, whereas that of medium-chain specific acyl-CoA dehydrogenase (*Mcad*), another gene related to fatty acid oxidation, was comparable (Fig. 3B). These results suggested that the hepatic lipid accumulation in FADS2$^{-/-}$ mice could be attributed to increased expression of SREBP-1c-dependent fatty acid synthesis genes. The activation of SREBPs requires proteolytic cleavage of the full-length protein to release the active form into the nucleus, which can then bind to their target promoter regions [25,26]. The ratio of cleaved to full-length SREBP-1 was significantly increased in the KO-DEF group (Fig. 3C), further suggesting that the deficiency of PUFAs with 20 carbons or more could have contributed to the accumulation of TAG in the liver by enhancing lipogenesis through the activation of SREBP-1.

It is known that the increase of cellular cholesterol or oxysterol, which is endogenously produced from cholesterol, inhibits SREBP cleavage. For example, side-chain oxysterols such as 27-hydroxycholesterol (27-OH) and 25-hydroxycholesterol (25-OH) inhibit the activation of SREBP-1 [27]. On the other hand, it has been recently reported that 4β-hydroxycholesterol (4β-OH) promotes SREBP-1c transcript and de novo lipogenesis [28]. The hepatic level of 27-OH and 4β-OH was increased in the KO-DEF group, whereas the difference of 25-OH level was not observed among three groups (Fig. 3D). Thus, the increase of 4β-OH in FADS2$^{-/-}$ mice may be correlated with increased gene expression of SREBP-1.

The impairment of VLDL secretion in FADS2 knockout mice fed a PUFA-deficient diet

Impaired secretion of VLDL inhibits the transfer of lipids from the liver to the plasma and is a possible cause of hepatic lipid accumulation. The hepatic expression of microsomal triglyceride transfer protein (*Mttp*), which plays important roles in VLDL assembly, did not significantly change in any of the three groups (Fig. S4A). There was also no difference in the protein level of hepatic apolipoprotein B-100 (apoB100), an essential component of VLDL, among the three groups (Fig. S4B). However, the protein level of plasma apoB100 in the KO-DEF group was reduced compared with those in the other two groups (Fig. 3E). In addition, the plasma TAG content was reduced in the KO-DEF group compared with that in the other two groups (Fig. 3F). The TAG content of the VLDL fraction in the KO-DEF group was also lower than that in both WT groups (Fig. 3G). It was suggested that VLDL secretion into the plasma was impaired in the liver of the KO-DEF group. It is reported that the decrease of arachidonic acid (20:4n-6) content in hepatic phosphatidylcholine (PC) leads to low membrane surface curvature and less ability for

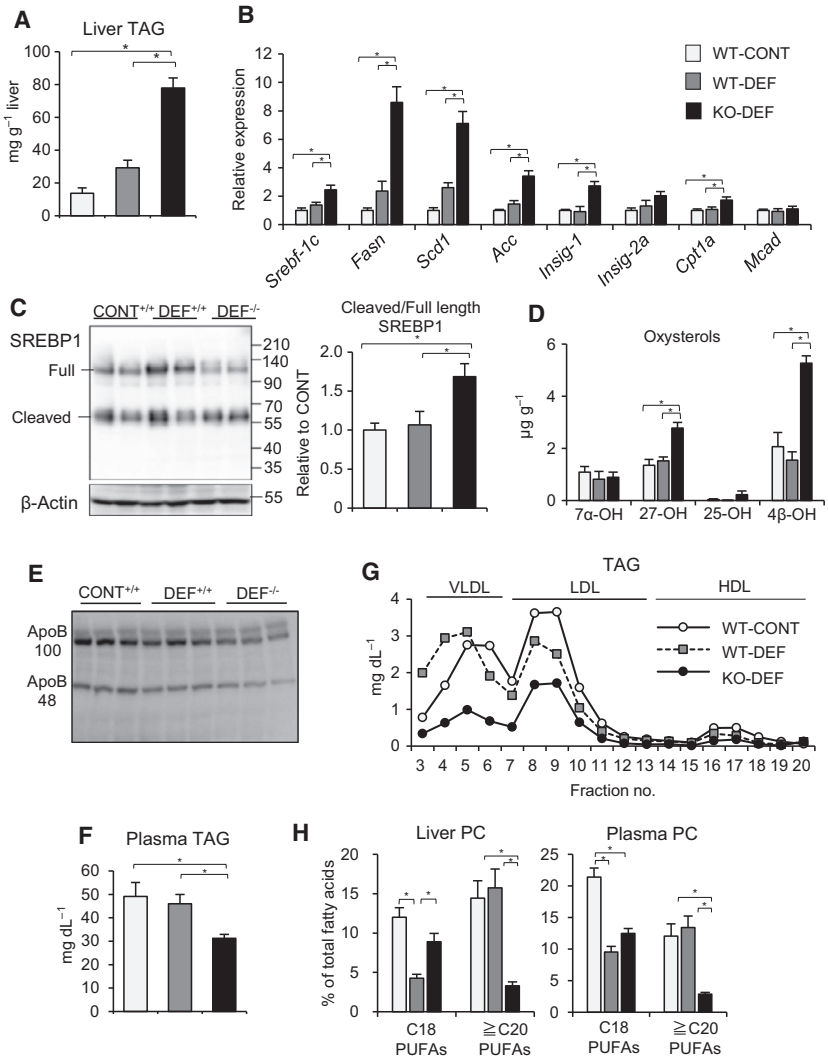

Fig. 3. PUFA-deficient FADS2$^{-/-}$ mice increased hepatic lipogenesis. (A) Liver TAG content was determined. (B) qRT-PCR examined hepatic expression of genes related to lipogenesis and lipolysis. Data are presented as mean values ± SE with 5–6 mice per group; $*P < 0.05$. (C) Full-length and cleaved SREBP-1 in the liver was examined by western blotting analysis. The ratio of the cleaved form (68 kDa) to full-length form (125 kDa) is indicated. (D) Hepatic oxysterol contents were determined by GC-MS. (E) Plasma ApoB proteins were examined by western blotting analysis. (F) TAG level in the plasma. (G) The plasma lipoprotein profile of TAG was analyzed by high-performance liquid chromatography (HPLC). (H) The levels of C18 PUFAs (18:2n-6 and 18:3n-3) and ≥ C20 PUFAs (20:3n-6, 20:3n-9, 20:4n-6, 20:5n-3, 22:5n-3, and 22:6n-3) in the phosphatidylcholine (PC) of the liver and the plasma. Data are presented as mean values ± SE with 5–6 mice per group; $*P < 0.05$.

TAG clustering, thereby impairing VLDL secretion [3,4]. When comparing the amounts of C18 PUFAs (18:2n-6 and 18:3n-3) in the liver and plasma PC, C18 PUFAs were reduced in both the WT-DEF and KO-DEF groups (Fig. 3H, Fig. S4C,D). However, the reduction of C18 PUFAs was more pronounced in the WT-DEF group than in the KO-DEF group. The amount of ≥ C20 PUFAs (20:3n-6, 20:3n-9, 20:4n-6, 20:5n-3, 22:5n-3, and 22:6n-3) of the liver and the plasma PC in the KO-DEF group markedly decreased compared to those in the other two groups. The amount of ≥ C20 PUFAs in the WT-DEF group was not lower than that in the WT-CONT group. These findings suggested that the decrease of ≥ C20 PUFAs in PC inhibited the secretion of VLDL and enhanced TAG accumulation in the liver.

Next, we investigated the hypothesis that hepatic TAG accumulation in the KO-DEF group was caused by increased release of free fatty acids (FFAs) from adipose tissue into the circulation and their uptake

into the liver. The hepatic gene expression of cluster of differentiation 36 (*Cd36*), a membrane protein that facilitates fatty acid uptake, in the KO-DEF group was higher than the WT-CONT group, while fatty acid transport protein 2 (*Fatp2*) and *Fatp5*, the major FATPs in the liver [29], were not upregulated in the liver of the KO-DEF group (Fig. S4E). Furthermore, the amount of total FFAs in the plasma and liver was not increased in the KO-DEF group (Fig. S4F,G), suggesting that FFAs mobilization may not be involved in hepatic lipid accumulation in FADS2$^{-/-}$ mice.

The mechanism of hepatic cholesterol accumulation in FADS2 knockout mice fed a PUFA-deficient diet

We unexpectedly found that cholesterol was accumulated in the FADS2$^{-/-}$ mouse liver (Fig. 4A). Cellular cholesterol levels are tightly regulated by the interplay among its de novo synthesis, uptake, export, and intracellular storage [30]. We then investigated the factors contributing to hepatic cholesterol accumulation in FADS2$^{-/-}$ mice. There are two pathways for cholesterol synthesis: the Bloch pathway and the Kandutsch-Russell pathway [31–33]. The intermediate sterols such as lanosterol and desmosterol were dramatically increased in the liver of the KO-DEF group, but lathosterol was not changed among the three groups (Fig. 4B), suggesting that cholesterol synthesis via the Bloch pathway was upregulated in the KO-DEF group. The mRNA expression levels of *Srebf-2* and its target genes, 3-hydroxy-3-methylglutaryl-CoA reductase (*Hmgcr*), farnesyl diphosphate synthase (*Fdps*), and lanosterol synthase (*Lss*), which are involved in the mevalonate pathway, were significantly elevated in the KO-DEF group compared with the other two groups. The mRNA expression levels of the squalene synthase (*Sqls*) and 24-dehydrocholesterol reductase (*Dhcr24*) did not differ among the three groups (Fig. 4C). These results suggested that the induction of cholesterogenesis could be one of the causes of cholesterol accumulation in the liver. Furthermore, there was no difference in the ratio of cleaved to full-length SREBP-2 among the three groups (Fig. 4D), suggesting that the activation of SREBP-2 did not contribute to the increased expression of genes involved in cholesterol synthesis.

Hepatic cholesterol secreted as part of VLDL returns to the liver as part of LDL, while excess peripheral cholesterol returns to the liver via high-density lipoprotein (HDL) and is excreted into the bile. The level of plasma cholesterol in the KO-DEF group was significantly lower than those in the two WT groups (Fig. 5A). Moreover, the cholesterol level of the HDL fraction in the KO-DEF group was also lower than those in the other two groups (Fig. 5B). This indicated that the low plasma cholesterol in the KO-DEF group might have been due to a lower cholesterol level in the HDL fraction. We therefore examined the expression of the genes involved in HDL metabolism, such as adenosine triphosphate binding cassette transporter 1 (*Abca1*), scavenger receptor class B type 1 (*Scarb1*), *Apo-a1*, and low-density lipoprotein receptor (*Ldlr*) (Fig. 5C). Of these, the expression levels of these genes *Abca1*, *Scarb1*, and *Apo-a1* did not differ significantly among the three groups, but the expression of *Ldlr* was upregulated in the KO-DEF group. We also examined the proprotein convertase subtilisin kexin 9 (*Pcsk9*), which impairs LDL clearance by promoting LDLR degradation. The hepatic gene expression and circulating level of PCSK9 were increased in the KO-DEF group (Fig. 5C,D). Therefore, it was not probable that the increase of *Ldlr* expression was the cause for hepatic cholesterol accumulation.

Hepatic expression levels of *Abcg5* and *Abcg8*, transporters for biliary excretion of cholesterol, were increased in the KO-DEF group (Fig. 5C), but the levels of biliary cholesterol and plasma TBA did not change among the three groups (Fig. 5E,F). Moreover, the expression levels of cholesterol 7 alpha-hydroxylase (*Cyp7a1*) and cholesterol 27 alpha-hydroxylase (*Cyp27a1*), which encode the rate-limiting enzymes in the bile acid synthetic pathway, did not show any difference between the WT and FADS2$^{-/-}$ mice (Fig. 5C). In addition, the intestinal expression of the genes involved in trans-intestinal cholesterol transport such as *Abcg8*, *Abca1,* and *Ldlr* was not different among the three groups (Fig. S5), and the expression of *Abcg5* in the intestine was decreased in the KO-DEF group. The expression of *Npc1l1*, which is critical for intestinal cholesterol absorption, also tended to decrease in the KO-DEF group ($P = 0.07$, vs. the WT-CONT group). From these results, it is unlikely that cholesterol excretion into bile and trans-intestinal cholesterol excretion are decreased in FADS2$^{-/-}$ mice.

Discussion

The dietary fatty acids n-3 and n-6 have been shown to suppress hepatic lipogenesis and have an inhibitory effect on hepatic steatosis [34], and the deficiency of PUFAs is known to induce hepatic steatosis. However, the importance of desaturation of PUFAs via FADS during PUFA deficiency remains unexplained. In the

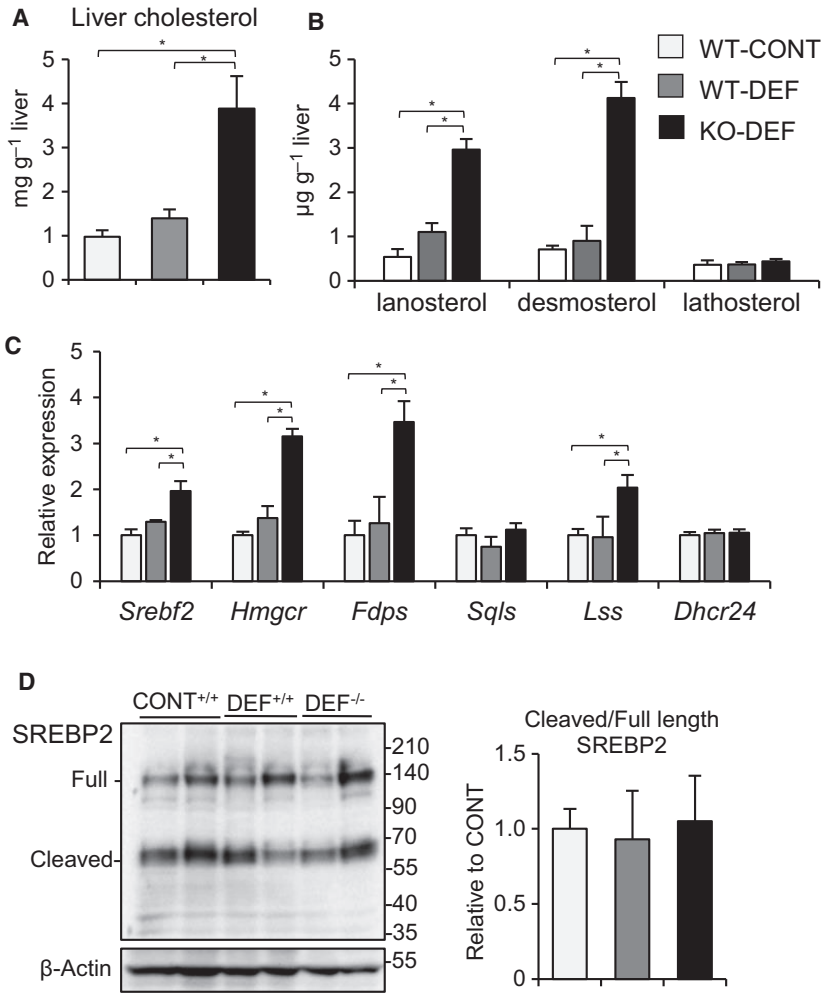

Fig. 4. The change in cholesterol synthesis in FADS2$^{-/-}$ mice fed a PUFA-deficient diet. Liver cholesterol (A) and the intermediate sterols (B) content were determined. (C) The levels of hepatic expression of genes related to cholesterol synthesis assessed by qRT-PCR. (D) Western blot results of full-length and cleaved SREBP-2 in the liver, and the ratio of the cleaved form (68 kDa) to the full-length form (125 kDa). Data are presented as mean values ± SE with 5–6 mice per group; *$P < 0.05$.

present study, we used mice deficient in FADS2, a rate-limiting enzyme for the production of ≥ C20 PUFAs from C18 PUFAs. The total amount of exogenous and endogenous ≥ C20 PUFAs in the liver of FADS2$^{-/-}$ mice fed a PUFA-deficient diet was reduced to less than one-fifth that of WT mice fed a control diet. To the best of our knowledge, the effect of sufficiency or deficiency of PUFAs on cholesterol metabolism has yet to be clarified. In addition, the effect of FADS2 deletion on hepatic cholesterol accumulation is still unknown [16]. In this study, FADS2$^{-/-}$ mice fed a PUFA-deficient diet elucidated pronounced hepatic accumulation of both TAG and cholesterol. Therefore, FADS2-mediated synthesis of ≥ C20 PUFA during PUFA depletion may have an inhibitory effect on hepatic steatosis.

This study demonstrated that the activation of SREBP-1, a master regulator transcription factor of lipogenesis, and induction of its target genes were involved in the increase of hepatic TAG in FADS2$^{-/-}$ mice fed a diet without PUFAs. This suggested that endogenous levels of ≥ C20 PUFAs such as arachidonic acid and DHA, but not C18 PUFAs, suppressed SREBP-1 activation. It is known that excess intracellular cholesterol inhibits SREBP cleavage [25], but SREBP-1 activation was observed despite the increase in hepatic cholesterol level of FADS2$^{-/-}$ mice. Moreover, impaired VLDL secretion also appeared to be involved in TAG accumulation in the liver of FADS2$^{-/-}$ mice. A study on mice with the lysophosphatidylcholine acyltransferase 3 (LPCAT3) knockout reported that a decrease in arachidonic acid content in phospholipids induced the inhibition of VLDL secretion [3,4]. It is known that ≥ C20 PUFAs in phospholipids play a crucial role in maintaining the structural and functional integrity of the cell membrane [35]. In our study, the factors involved in VLDL secretion, including TAG level in VLDL particles, apoB protein,

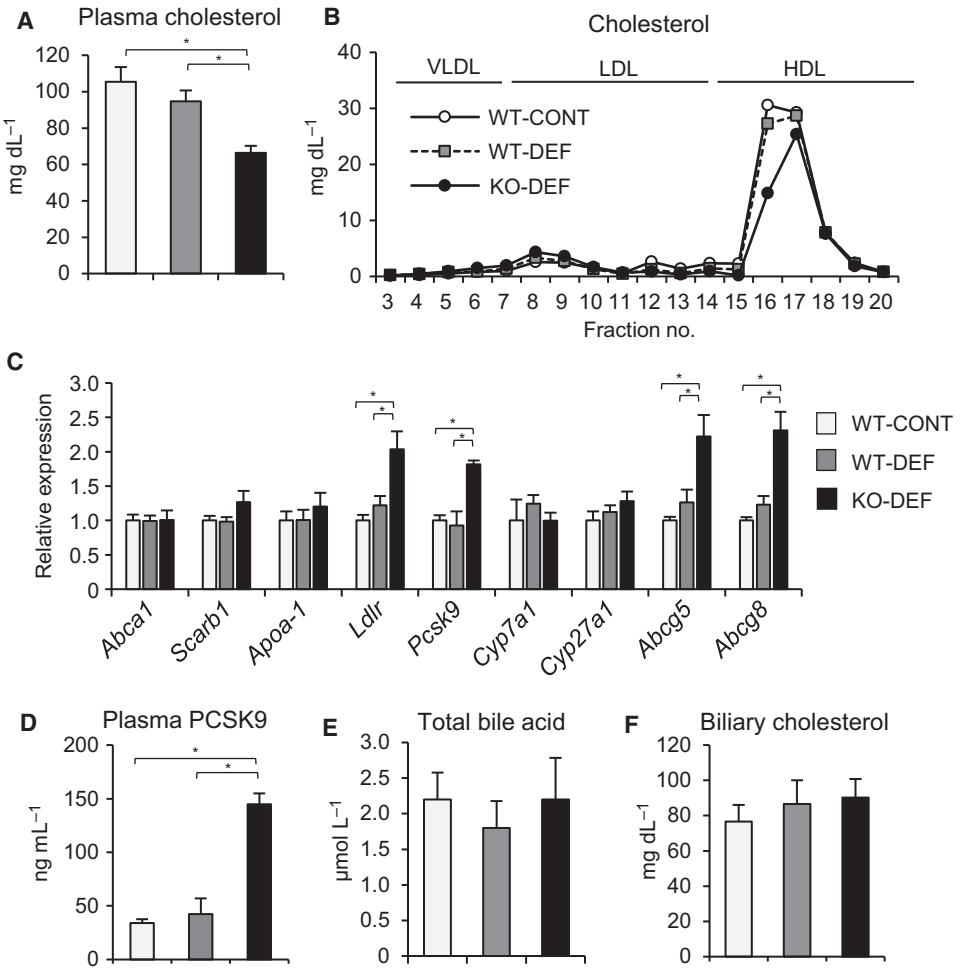

Fig. 5. The change in cholesterol metabolism in FADS2$^{-/-}$ mice fed a PUFA-deficient diet (A) Plasma cholesterol level. (B) High-performance liquid chromatography results of plasma lipoprotein profile of cholesterol. (C) Hepatic expression levels of genes involved in cholesterol transport assessed by qRT-PCR. (D) Plasma PCSK9 content was determined by ELISA. (E) Total bile acid content in the plasma and (F) cholesterol level in the bile were examined. Data are presented as mean values ± SE with 5–6 mice per group; *$P < 0.05$.

and ≥ C20 PUFAs in phospholipid, were reduced in FADS2$^{-/-}$ mice, while such reductions were not observed in WT mice. Taken together, these results suggested that the depletion of HUFAs in phospholipids might prevent the normal secretion of VLDL from the liver.

In this study, FADS2$^{-/-}$ mice fed the deficient diet showed a significantly increased expression of genes involved in the mevalonate pathway of cholesterol synthesis, suggesting that depletion of ≥ C20 PUFAs in the liver resulted in the upregulation of cholesterol synthesis. Furthermore, our study confirmed the activation of SREBP-1, but not SREBP-2, a transcription factor for cholesterol synthesis genes, in FADS2$^{-/-}$ mice. This was consistent with the previous findings on the increased intracellular level of PUFAs which were more effective at inhibiting SREBP-1 activation than SREBP-2 activation [11,36,37]. While in the present study, we could not decipher the mechanism underlying the regulation of genes involved in cholesterol production in mice deficient in ≥ C20 PUFAs, hepatic cholesterol accumulation in FADS2$^{-/-}$ mice may be caused by a SREBP-2-independent increase of cholesterol synthesis. In addition, this study was not able to confirm any changes in gene expression that are responsible for trans-intestinal cholesterol excretion in FADS2$^{-/-}$ mice; however, the quantification of fecal neutral sterol will further clarify the contribution of trans-intestinal cholesterol excretion to the increase in hepatic cholesterol content. Further studies are needed to elucidate the detailed mechanism of hepatic cholesterol accumulation in the HUFA-deficient mice.

FADS2$^{-/-}$ mice fed a PUFA-deficient diet had reduced plasma cholesterol and low cholesterol levels in the HDL fraction compared with WT mice, suggesting that the deficiency of HUFAs caused the dysfunction of reverse cholesterol transport (RCT). Overexpression of a gene involved in HDL production, which plays an important role in RCT, has been reported to ameliorate cholesterol accumulation in the liver of nonalcoholic fatty liver disease (NAFLD) model mice [38]. Therefore, there is a possibility that the reduction of RCT in FADS2$^{-/-}$ mice contributed to the accumulation of hepatic cholesterol. The SREBP-1 promoter contains an LXR response element, demonstrating the potential for lipid regulation via LXR [39]. Importantly, LXR, a pivotal regulator of cholesterol homeostasis, is also reported to be negatively regulated by PUFAs [11]. The expression of the LXR target gene *Abca1* was unchanged in FADS2$^{-/-}$ mice with severely reduced ≥ C20 PUFAs, whereas the expression levels of other LXR target genes *Abcg5/8* were increased. Considering this inconsistency in the expression pattern of LXR target genes, further studies should be performed to determine whether HUFA deficiency leads to the activation of LXR in this model.

HUFAs play an important role in controlling hepatic TAG and cholesterol deposits and are maintained by FADS2-mediated synthesis, even during PUFA deficiency. This study showed that the hepatic accumulation of cholesterol and TAG occurred when there was a deficiency of PUFAs with 20 or more carbons. It is known that people with a single-nucleotide polymorphism of *FADS* have low plasma HUFA levels [40,41]. In addition, decreased FADS1 and FADS2 activity has been implicated in NAFLD [42]. Therefore, it may be necessary for individuals with dysregulated HUFA synthesis to supplement their diet with a sufficient amount of ≥ C20 PUFAs to alleviate the pathogenesis and progression of NAFLD. Further studies are required to fully understand the mechanism of hepatic neutral lipid accumulation induced by HUFA deficiency.

Acknowledgements

This research was supported by grants from the Ministry of Education, Culture, Sports, Science and Technology (MEXT)/Japanese Society for the Promotion of Sport Grants-in-Aid for Scientific Research (KAKENHI) (17K00848 and 20K02383 to II, 15H06600, 18K16246, and 21K08565 to HCLO), the Mishima Kaiun Memorial Foundation (II), and Research Grants from the Takeda Science Foundation (HCLO).

Author contributions

YH, HCLO, YF, and II designed the research. YH and II conducted the research. YH and II performed experiments and analyzed the data. HCLO, EN, NT, and TY provided the animals. YH, HCLO, and II wrote the paper.

Data accessibility

The data that support the findings of this study are available in the figures and the supplementary material of this article.

References

1 Mead JF and Slaton WH Jr (1956) Metabolism of essential fatty acids, III. Isolation of 5,8,11-eicosatrienoic acid from fat-deficient rats. *J Biol Chem* **219**, 705–709.
2 Ichi I, Kono N, Arita Y, Haga S, Arisawa K, Yamano M, Fujiwara Y and Arai H (2014) Identification of genes and pathways involved in the synthesis of Mead acid (20:3n–9), an indicator of essential fatty acid deficiency. *Biochim Biophys Acta-Mol Cell Biol Lipids* **1841**, 204–213.
3 Hashidate-Yoshida T, Harayama T, Hishikawa D, Morimoto R, Hamano F, Tokuoka SM, Eto M, Tamura-Nakano M, Yanobu-Takanashi R, Mukumoto Y *et al.*, (2015) Fatty acid remodeling by LPCAT3 enriches arachidonate in phospholipid membranes and regulates triglyceride transport. *eLife* **4**, e06328.
4 Rong X, Wang B, Dunham M-M, Hedde P-N, Wong J-S, Gratton E and Tontonoz P (2015) Lpcat3-dependent production of arachidonoyl phospholipids is a key determinant of triglyceride secretion. *eLife* **4**, e06557.
5 Hayashi Y, Shimamura A, Ishikawa T, Fujiwara Y and Ichi I (2018) FADS2 inhibition in essential fatty acid deficiency induces hepatic lipid accumulation via impairment of very low-density lipoprotein (VLDL) secretion. *Biochem Biophys Res Commun* **496**, 549–555.
6 Patel P, Cossette C, Anumolu J-R, Gravel S, Lesimple A, Mamer O-A and Powell W-S (2008) Structural requirements for Activation of the 5-Oxo-6E,8Z, 11Z,14Z-eicosatetraenoic acid (5-Oxo-ETE) Receptor: identification of a mead acid metabolite with potent agonist activity. *J Pharmacol Exp Ther* **325**, 698–707.
7 Hsu L-C, Wen W-H, Chen H-M, Lin H-T, Chiu C-M and Wu H-C (2013) Evaluation of the anti-inflammatory activities of 5,8,11-cis-Eicosatrienoic acid. *Food Nutr Sci* **4**, 113–119.

8 Simopoulos AP (1999) Essential fatty acids in health and chronic disease. *Am J Clin Nutr* **70**, 560S–569S.
9 Jorgensen EA and Holman RT (1958) Essential fatty acid deficiency: content of polyenoic acids in testes and heart as an indicator of essential fatty acid status. *J Nutr* **65**, 633–641.
10 Innis S-M (1991) Essential fatty acids in growth and development. *Prog Lipid Res* **30**, 39–103.
11 Ou J, Tu H, Shan B, Luk A, DeBose-Boyd RA, Bashmakov Y, Goldstein JL and Brown MS (2001) Unsaturated fatty acids inhibit transcription of the sterol regulatory element-binding protein-1c (SREBP-1c) gene by antagonizing ligand-dependent activation of the LXR. *Proc Natl Acad Sci USA* **98**, 6027–6032.
12 Werner A, Havinga R, Bos T, Bloks VW, Kuipers F and Verkade HJ (2005) Essential fatty acid deficiency in mice is associated with hepatic steatosis and secretion of large VLDL particles. *Am J Physiol Gastrointest Liver Physiol* **288**, G1150–G1158.
13 Subramanian S, Goodspeed L, Wang S, Kim J, Zeng L, Ioannou GN and Chait A (2011) Dietary cholesterol exacerbates hepatic steatosis and inflammation in obese LDL receptor-deficient mice. *J Lipid Res* **52**, 1626–1635.
14 Stoffel W, Holz B, Jenke B, Binczek E, Günter RH, Kiss C and Addicks K (2008) D6- desaturase (FADS2) deficiency unveils the role of u3- and u6-polyunsaturated fatty acids. *EMBO J* **27**, 2281–2292.
15 Stroud CK, Nara TY, Roqueta-Rivera M, Radlowski EC, Lawrence P, Zhang Y and Nakamura MT (2009) Disruption of FADS2 gene in mice impairs male reproduction and causes dermal and intestinal ulceration. *J Lipid Res* **50**, 1870–1880.
16 Stoffel W, Hammels I, Jenke B, Binczek E, Schmidt Soltau I, Brodesser S, Odenthal M and Thevis M (2013) Obesity resistance and deregulation of lipogenesis in Δ6-fatty acid desaturase (FADS2) deficiency. *EMBO Rep* **15**, 110–120.
17 Wang H, Yang H, Shivalila CS, Dawlaty MM, Cheng AW, Zhang F and Jaenisch R (2013) One-step generation of mice carrying mutations in multiple genes by CRISPR/Cas-mediated genome engineering. *Cell* **153**, 1–9.
18 Whitten WK (1971) Embryo medium: nutrient requirements for the culture of preimplantation embryos in vitro. *Adv Biosci* **6**, 129–141.
19 Bligh EG and Dyer WJ (1959) A rapid method of total lipid extraction and purification. *Can J Biochem Physiol* **37**, 911–917.
20 Arisawa K, Ichi I, Yasukawa Y, Sone Y and Fujiwara Y (2013) Changes in the phos- pholipid fatty acid composition of the lipid droplet during the differentiation of 3T3-L1 adipocytes. *J Biochem* **154**, 281–289.
21 Tomoyori H, Kawata Y, Higuchi T, Ichi I, Sato H, Sato M, Ikeda I and Imaizumi K (2004) Phytosterol oxidation products are absorbed in the intestinal lymphatics in rats but do not accelerate atherosclerosis in apolipoprotein E-deficient mice. *J Nutr* **134**, 1690–1696.
22 Dzeletovic S, Breuer O, Lund E and Diczfalusy U (1995) Determination of cholesterol oxidation products in human plasma by isotope dilution-mass spectrometry. *Anal Biochem* **225**, 73–80.
23 Usui S, Hara Y, Hosaki S and Okazaki M (2002) A new on-line dual enzymatic method for simultaneous quantification of cholesterol and triglycerides in lipoproteins by HPLC. *J Lipid Res* **43**, 805–814.
24 Goldstein JL, DeBose-Boyd RA and Brown MS (2006) Protein sensors for membrane sterols. *Cell* **124**, 35–46.
25 Brown MS and Goldstein JL (2008) Cholesterol feedback: from Schoenheimer's bottle to Scap's MELADL. *J Lipid Res* **50**(Suppl), S15–S27.
26 Radhakrishnan A, Goldstein JL, McDonald JG and Brown MS (2008) Switch-like control of SREBP-2 transport triggered by small changes in ER cholesterol: A delicate balance. *Cell Metab* **8**, 512–521.
27 Radhakrishnan A, Ikeda Y, Kwon HJ, Brown MS and Goldstein JL (2007) Sterol-regulated transport of SREBPs from endoplasmic reticulum to Golgi: oxysterols block transport by binding to Insig. *Proc Natl Acad Sci USA* **104**, 6511–6518.
28 Moldavski O, Zushin P-JH, Berdan CA, Eijkeren RJV, Jiang X, Qian M, Ory DS, Covey DF, Nomura DK, Stahl A *et al.*, (2021) 4β-Hydroxycholesterol is a prolipogenic factor that promotes SREBP1c expression and activity through the liver X receptor. *J Lipid Res* **23**, 100051.
29 Hirsch D, Stahl A and Lodish HF (1998) A family of fatty acid transporters conserved from Mycobacterium to man. *Proc Natl Acad Sci USA* **95**, 8625–8629.
30 Luo J, Yang H and Song B (2019) Mechanisms and regulation of cholesterol homeostasis. *Nat Rev Mol Cell Biol* **21**, 225–245.
31 Bloch K (1965) The biological synthesis of cholesterol. *Science* **150**, 19–28.
32 Kandutsch AA and Russell AE (1960) Preputial gland tumor sterols. 2. The identification of 4 alpha-methyl-Delta 8-cholesten-3 beta-ol. *J Biol Chem* **235**, 2253–2255.
33 Kandutsch AA and Russell AE (1960) Preputial gland tumor sterols. 3. A metabolic pathway from lanosterol to cholesterol. *J Biol Chem* **235**, 2256–2261.
34 Musa-Veloso K, Venditti C, Lee HY, Darch M, Floyd S, West S and Simon R (2018) Systematic review and meta-analysis of controlled intervention studies on the effectiveness of long-chain omega-3 fatty acids in patients with nonalcoholic fatty liver disease. *Nutr Rev* **76**, 581–602.
35 Leifert WR, Jahangiri A and McMurchie EJ (2000) Membrane fluidity changes are associated with the

antiarrhythmic effects of docosahexaenoic acid in adult rat cardiomyocytes. *J Nutr Biochem* **11**, 38–44.
36 Takeuchi Y, Yahagi N, Izumida Y, Nishi M, Kubota M, Teraoka Y, Yamamoto T, Matsuzaka T, Nakagawa Y, Sekiya M *et al.*, (2010) Polyunsaturated fatty acids selectively suppress sterol regulatory element-binding protein-1 through proteolytic processing and Autoloop regulatory circuit. *J Biol Chem* **285**, 11681–11691.
37 Kim H, Takahashi M and Ezaki O (1999) Fish oil feeding decreases mature sterol regulatory element-binding protein 1 (SREBP-1) by down-regulation of SREBP-1c mRNA in mouse liver. *J Biol Chem* **274**, 25892–25898.
38 Kasbi Chadli F, Nazih H, Krempf M, Nguyen P and Ouguerram K (2013) Omega 3 fatty acids promote macrophage reverse cholesterol transport in hamster fed high fat diet. *PLoS One* **8**, e61109.
39 Repa JJ (2000) Regulation of mouse sterol regulatory element-binding protein-1c gene (SREBP-1c) by oxysterol receptors, LXRalpha and LXRbeta. *Genes Dev* **14**, 2819–2830.
40 Cormier H, Rudkowska I, Lemieux S, Couture P, Julien P and Vohl M (2014) Effects of FADS and ELOVL polymorphisms on indexes of desaturase and elongase activities: Results from a pre-post fish oil supplementation. *Genes Nutr* **9**, 437.
41 Schaeffer L, Gohlke H, Müller M, Heid IM, Palmer LJ and Kompauer I (2006) Common genetic variants of the FADS1 FADS2 gene cluster and their reconstructed haplotypes are associated with the fatty acid composition in phospholipids. *Hum Mol Genet* **15**, 1745–1756.
42 Araya J, Rodrigo R, Pettinelli P, Araya AV, Poniachik J and Videla LA (2010) Decreased liver fatty acid Δ-6 and Δ-5 Desaturase activity in obese patients. *Obesity* **18**, 1460–1463.

Supporting information

Additional supporting information may be found online in the Supporting Information section at the end of the article.

Fig. S1. Generation of FADS2$^{-/-}$ mice using the CRISPR/Cas9 system. Generation of FADS2$^{-/-}$ mice using the CRISPR/Cas9 system.

Fig. S2. Fatty acid composition in the plasma of FADS2-deficient mice fed a PUFA-deficient diet was determined by GC-MS.

Fig. S3. Liver weight and fatty acid composition in FADS2−/− mice fed a control or PUFA-deficient diet.

Fig. S4. Hepatic factors involved in VLDL secretion and free fatty acid (FFA) transport.

Fig. S5. The change of expression of genes involving trans-intestinal cholesterol excretion.